YUCCA Genes Are Expressed in Response to Leaf Adaxial-Abaxial Juxtaposition and Are Required for Leaf Margin Development[1][W]

Wei Wang, Ben Xu[2], Hua Wang, Jiqin Li, Hai Huang, and Lin Xu*

National Laboratory of Plant Molecular Genetics, Shanghai Institute of Plant Physiology and Ecology, Shanghai Institutes for Biological Sciences, Chinese Academy of Sciences, Shanghai 200032, China

During leaf development, the formation of leaf adaxial-abaxial polarity at the primordium stage is crucial for subsequent leaf expansion. However, little is known about the genetic control from polarity establishment to blade outgrowth. The leaf margin, comprising elongated margin cells and hydathodes, is thought to affect leaf expansion. Here, we show that mutants with defective leaf polarity or with loss of function in the multiple auxin-biosynthetic *YUCCA* (*YUC*) genes exhibited a similar abnormal leaf margin and less-expanded leaves. Leaf margins of these mutants contained fewer hydathodes and an increased number of cell patches in which the patterns of epidermal cells resembled those of hydathodes. The previously characterized leaf-abaxialized *asymmetric leaves2* (*as2*) *revoluta* (*rev*) and leaf-adaxialized *kanadi1* (*kan1*) *kan2* double mutants both produce finger-shaped, hydathode-like protrusions on adaxial and abaxial leaf surfaces, respectively. *YUC*s are required for formation of the protrusions, as those produced by *as2 rev* and *kan1 kan2* were absent in the *yuc1 yuc2 yuc4* triple mutant background. Expressions of *YUC1*, *YUC2*, and *YUC4* were spatially regulated in the leaf, being associated with hydathodes in wild-type leaves and protrusions on *as2 rev* and *kan1 kan2* leaves. In addition, inhibition of auxin transport by treatment of seedlings with *N*-(1-naphtyl) phtalamic acid or disruption of the auxin gradient by transforming plants with the *35S*:*YUC1* construct also blocked leaf margin development. Collectively, our data show that expressions of *YUC*s in the leaf respond to the adaxial-abaxial juxtaposition, and that the activities of auxin mediate leaf margin development, which subsequently promotes blade outgrowth.

Leaf primordia of higher plants derive from the peripheral zone of the shoot apical meristem. After initiation of the primordia, leaves are patterned along adaxial-abaxial, proximodistal, and mediolateral axes. The pioneering microsurgical experiments carried out by Sussex, and the results from subsequent studies on the establishment of leaf polarity and blade outgrowth, have led to several important proposals concerning leaf development: (1) leaf adaxial cell differentiation is triggered by a signal (now termed the Sussex signal) originating from the shoot apical meristem, whereas abaxial cell differentiation is a default process; (2) leaf primordia perceive the signal and initiate the establishment of leaf polarity at or before the P1 leaf developmental stage; and (3) the juxtaposition of the leaf adaxial and abaxial domains directs blade outgrowth along the mediolateral axis (Sussex, 1954, 1955; Hudson, 1999; Eshed et al., 2001; Reinhardt et al., 2005).

During the last decade, a great number of leaf adaxial- and abaxial-promoting factors have been identified (Kidner and Timmermans, 2007; Xu et al., 2007; Bowman and Floyd, 2008; Szakonyi et al., 2010). Some leaf polarity mutants show trumpet- or lotus-shaped leaves, which reflect a loss of leaf expansion in the proximal part (Waites and Hudson, 1995; McConnell and Barton, 1998; Emery et al., 2003; Xu et al., 2003). In extreme cases, complete loss of either adaxial or abaxial identity results in filamentous leaves without blade outgrowth (Waites and Hudson, 1995; McConnell and Barton, 1998; Emery et al., 2003; Xu et al., 2003). Some leaf polarity mutants show another kind of phenotype, with many finger-shaped protrusions on the abaxial surface, as in *kanadi1* (*kan1*) *kan2* and *auxin response factor3 auxin response factor4* double mutants (Eshed et al., 2001; Pekker et al., 2005), or on the adaxial side, as in *asymmetric leaves2* (*as2*) *revoluta* (*rev*) double mutant (Fu et al., 2007). Leaves of all these double mutants do not expand normally. The formation of protrusions was thought to be caused by the ectopic adaxial-abaxial juxtaposition on the lamina and activation of ectopic blade outgrowth (Waites and Hudson, 1995; Eshed et al., 2001, 2004; Fu et al., 2007). Based on the results described above, leaf adaxial-abaxial polarity appears to be an important factor for normal blade outgrowth. However, how leaf

[1] This work was supported by the Chief Scientist Program of the Shanghai Institutes for Biological Sciences and the Chinese National Scientific Foundation (grant nos. 31071064 and 90717107), and partly supported by National Basic Research Program of China (973 Program) 2012CB910503.

[2] Present address: Department of Internal Medicine, Division of Molecular Medicine and Genetics, University of Michigan, Ann Arbor, MI 48109–2200.

* Corresponding author; e-mail xulin01@sibs.ac.cn.

The author responsible for distribution of materials integral to the findings presented in this article in accordance with the policy described in the Instructions for Authors (www.plantphysiol.org) is: Lin Xu (xulin01@sibs.ac.cn).

[W] The online version of this article contains Web-only data.
www.plantphysiol.org/cgi/doi/10.1104/pp.111.186395

adaxial-abaxial polarity influences blade outgrowth is poorly understood.

Previous studies suggested that correct blade outgrowth depends on the formation of a normal leaf margin, a process that is controlled by meristematic cells along the leaf margin (Poethig and Sussex, 1985; Donnelly et al., 1999). Several studies also demonstrated that auxin is generated in the leaf margin and forms a gradient to facilitate blade outgrowth (Mattsson et al., 1999; Aloni et al., 2003; Scanlon, 2003; Zgurski et al., 2005). In addition, *YABBY* genes were thought to be required for the adaxial and abaxial juxtaposition-mediated blade outgrowth (Eshed et al., 2004). Recent findings have demonstrated that *YABBY* functions are required for leaf margin formation, leaf marginal auxin flow, and other laminar-specific programs to direct blade outgrowth (Sarojam et al., 2010), providing important information in elucidating the relationships between auxin and leaf margin formation and blade outgrowth.

Auxin is one of the major phytohormones in higher plants and has wide-ranging effects on plant growth and development. Auxin biosynthesis, polar transport, and signaling all critically affect various processes in plant development (Woodward and Bartel, 2005; Benjamins and Scheres, 2008; Vanneste and Friml, 2009). The genes in the *YUCCA* (*YUC*) family of Arabidopsis (*Arabidopsis thaliana*) encode flavin monooxygenase-like enzymes that catalyze the rate-limiting step in Trp-dependent auxin biosynthesis. These enzymes play important roles in local auxin biosynthesis (Zhao et al., 2001). The *YUC* family contains 11 members, and when four of these were mutated (the quadruple mutant *yuc1 yuc2 yuc4 yuc6*), the mutant plants showed severe auxin-deficient phenotypes with narrow leaves (Cheng et al., 2006). In addition, the *YUC*-controlled leaf developmental pathway acts synergistically with auxin polar transport (Cheng et al., 2007). In this study, we show that leaf adaxial-abaxial polarity is required for normal expression of several *YUC* genes, and that *YUC* functions are important in leaf margin development and blade outgrowth.

RESULTS

Characterization of the Arabidopsis Leaf Margin

The margin of a mature Arabidopsis rosette leaf (Fig. 1A) contains morphologically elongated margin cells (Fig. 1B) and hydathodes (Fig. 1C). The margin cells are straight and narrow (Fig. 1B, red arrows). The hydathode epidermis comprises irregularly shaped cells (Fig. 1C, yellow arrowheads) mixed with stomata (Fig. 1C, green arrows). As shown in the first-pair rosette leaves, the young leaf primordium comprises cells of homogenous shape (Fig. 1, D and E), with no margin cells or hydathodes. The margin becomes evident when cells begin to differentiate along the adaxial-abaxial axis, with elongating margin cells appearing at the leaf primordium at 4 d after germination (DAG; Fig. 1F). Hydathodes begin to develop on 6-DAG leaves, initially in the proximal part of the blade (Fig. 1G) among the morphologically distinct elongating margin cells (Fig. 1H). The cell types at the leaf tip are similar to those of a hydathode (Fig. 1I). In wild-type Columbia-0 (Col-0) plants, the margin of a mature leaf usually bears two to 16 hydathodes distributed all along the margin. The number of hydathodes on individual leaves differs largely with leaf size and its position of initiation (Fig. 1J). Occasionally, the leaf margin produces a few cell patches, most of which are associated with hydathodes (Fig. 1K). These patches contain only a few irregularly shaped epidermal cells and stomata (Fig. 1L), similar to those on the top part of hydathodes (Fig. 1C).

Leaf Margin Formation Responds to Adaxial-Abaxial Polarity

A leaf with complete loss of either adaxial or abaxial identity forms a radially symmetrical structure (Sussex, 1954, 1955; Waites and Hudson, 1995; McConnell and Barton, 1998; Emery et al., 2003; Xu et al., 2003; Reinhardt et al., 2005). Such an unexpanded leaf usually lacks a leaf margin. To better understand how leaf adaxial-abaxial polarity affects leaf margin formation, we analyzed leaf margins of the polarity-defective double mutants *as2-1 rev-1* and *kan1-11 kan2-5*, in which the adaxial-abaxial polarity in most leaves is severely affected but not completely lost (Eshed et al., 2004; Fu et al., 2007; Wu et al., 2008). The *as2-1*, *rev-1*, *kan1-11*, and *kan2-5* single mutants do not show obvious leaf polarity defects, whereas both *as2-1 rev-1* and *kan1-11 kan2-5* double mutants exhibit not only altered leaf polarity, but also a defective leaf margin (see below).

Scanning electron microscopy (SEM) analysis revealed that leaves of both *as2-1 rev-1* and *kan1-11 kan2-5* were smaller than fully expanded leaves of the wild type and those of the corresponding single mutants (data not shown). The double mutants also had lobes on their rosette leaves (Fig. 2, A and D). Although the margins of the *as2-1 rev-1* and *kan1-11 kan2-5* leaves contained hydathodes and elongated margin cells, the leaves of the double mutants had fewer hydathodes than the wild type (Fig. 2G; Supplemental Fig. S1) and there were many more margin cell patches than in the wild type (Fig. 2, B, E, and H). Whereas most cell patches were located near hydathodes in wild-type leaves, cell patches in the double mutants could occur anywhere among the margin cells (Fig. 2I).

In addition to the abnormal leaf margin, both double mutants produced finger-shaped protrusions. These were observed on the adaxial side of late-appearing leaves of *as2-1 rev-1* (Fig. 2, A and C) and on the abaxial side of *kan1-11 kan2-5* leaves (Fig. 2, D and F), as previously reported (Eshed et al., 2004; Fu et al., 2007; Wu et al., 2008). More detailed SEM observations

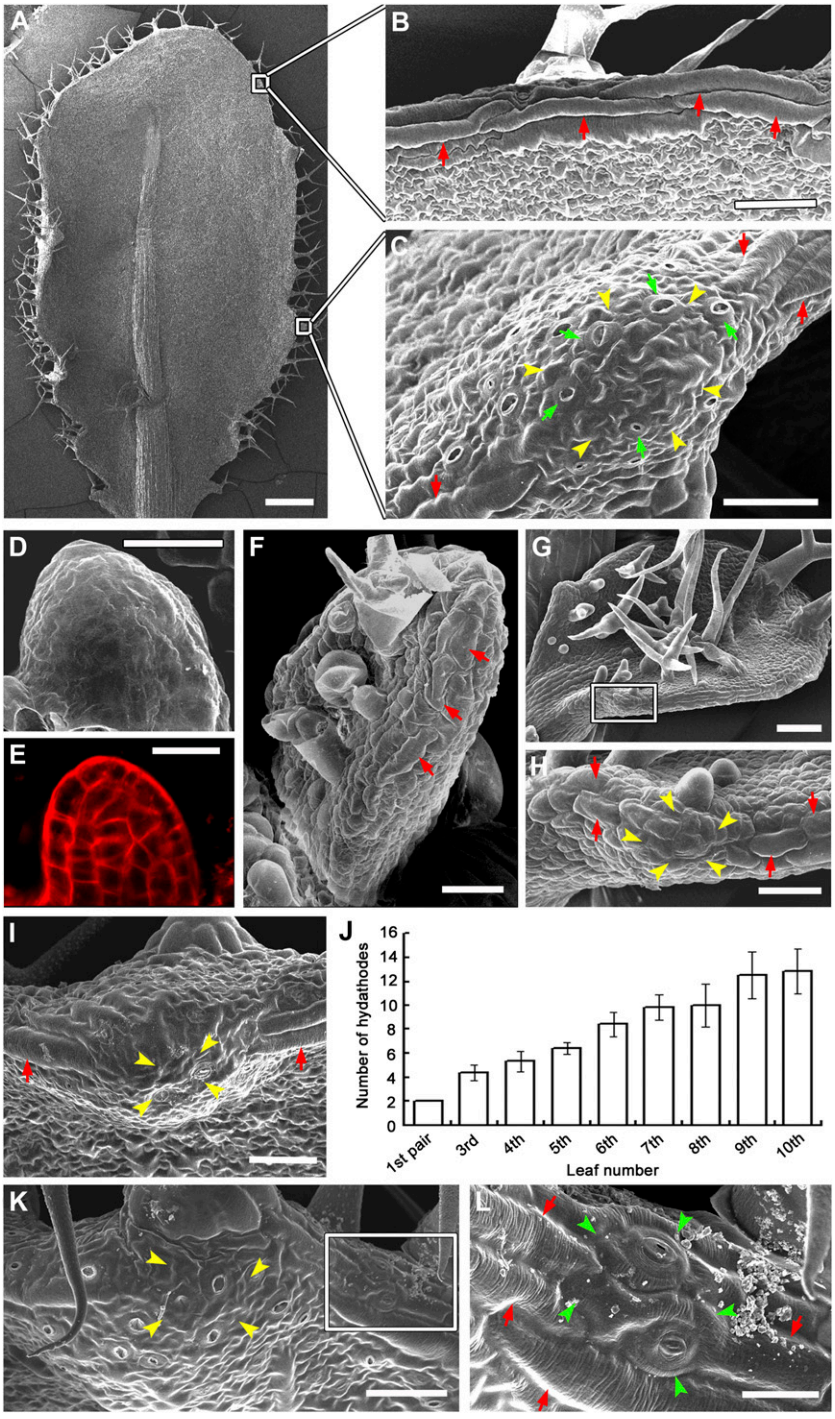

Figure 1. Characterization of the Arabidopsis leaf margin. A, A mature wild-type leaf. B, The boxed region in A at higher magnification. C, A hydathode in the boxed region in A with irregularly shaped epidermal cells (yellow arrowheads) and stomata (green arrows). D and E, A 2-DAG leaf primordium examined by SEM (D) or confocal microscopy after FM4-64 staining (E). F, A 4-DAG young leaf. Red arrows indicate the elongating margin cells. G, A 6-DAG leaf with hydathodes beginning to form. H, A newly formed hydathode in the boxed region in G, showing the immature hydathode epidermal cells (yellow arrowheads) and the elongating margin cells (red arrows). I, A leaf tip with epidermal cells (yellow arrowheads) similar to those on hydathodes. J, The numbers of hydathodes in different sequential leaves in wild-type Col-0. $n = 20$ for the first-pair leaves; $n = 10$ for the other leaves. Error bars represent the SE. K, Leaf margin also contains cell patches structure, most of which are located close to hydathodes (yellow arrowheads). L, Close-up of the boxed region in K to show a cell patch (green arrowheads). Red arrows indicate elongated margin cells. Scale bars: 1 mm in A; 50 μm in B, C, G, I, and K; 20 μm in D to F, H, and L.

revealed that the top part of these finger-shaped structures was covered with irregularly shaped small cells mixed with stomata (Fig. 2, C and F, yellow arrowheads), resembling a hydathode (Fig. 1C), whereas the lower part contained elongated cells that resembled leaf margin cells (Eshed et al., 2004; Fig. 2, C and F, red arrows). We also analyzed the internal structure of these protrusions by differential interference contrast microscopy. Our data revealed that the protrusions in both *as2-1 rev-1* and *kan1-11 kan2-5* contained epithem-like structures (Fig. 2, K and L) that were connected to vascular endings, just like those in hydathodes in the wild type (Fig. 2J). These results suggest that the finger-shaped protrusions on the leaves of polarity-defective mutants are hydathode-like structures, and cell patches in both wild type and leaf polarity mutants might represent hydathodes lacking protrusions and internal structures.

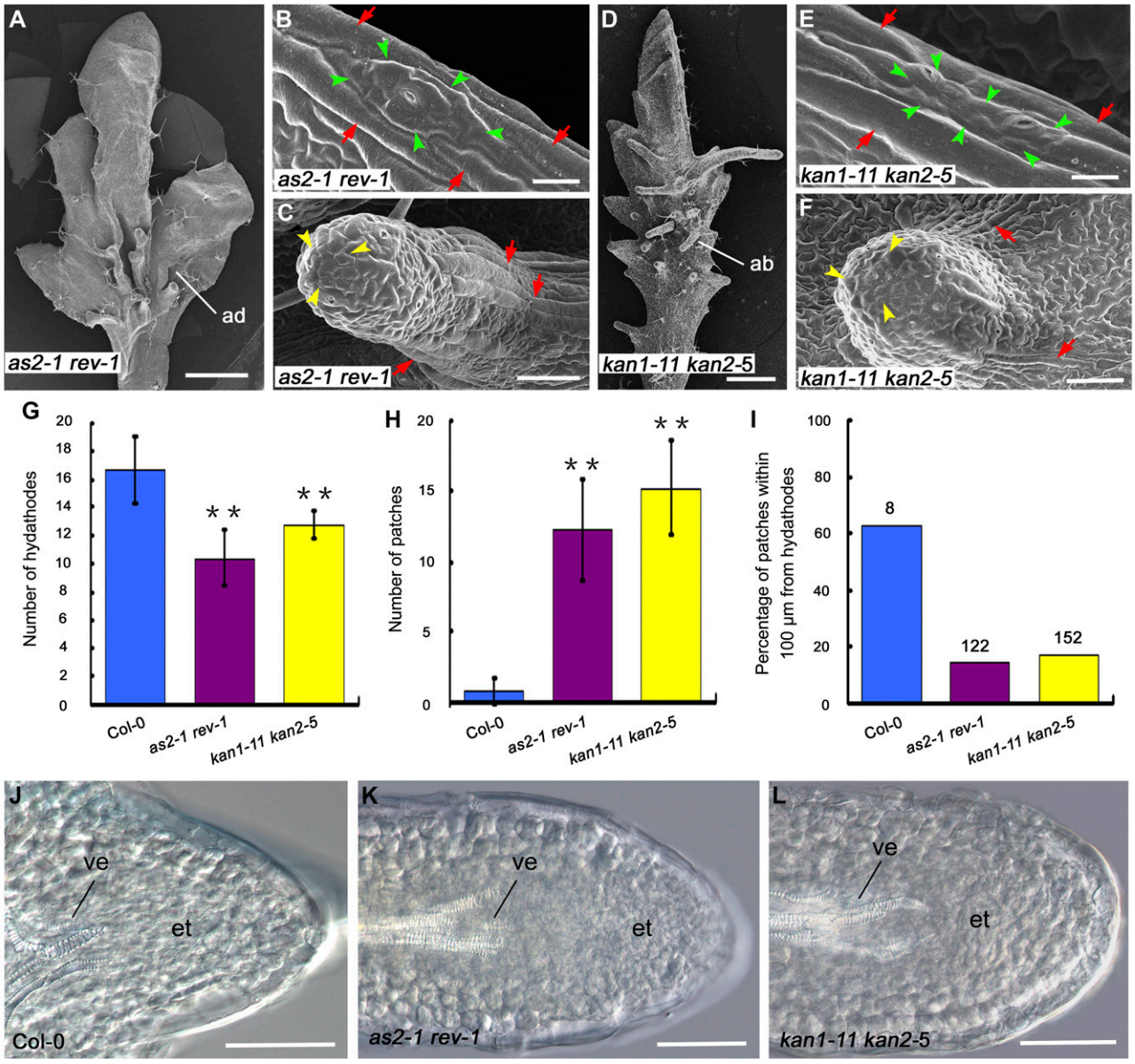

Figure 2. Leaf margin formation responds to the adaxial-abaxial polarity. A and D, A 10th leaf of *as2-1 rev-1* (A) and a sixth leaf of *kan1-11 kan2-5* (D) showing finger-shaped protrusions on the adaxial (A) and the abaxial (D) sides, respectively. B and E, Among elongated margin cells (red arrows) of the a*s2-1 rev-1* (B) and *kan1-11 kan2-5* (E) leaves, the cell patches (green arrowheads) were often seen. C and F, Close-ups of protrusions on *as2-1 rev-1* (C) and *kan1-11 kan2-5* (F) leaves. Yellow arrowheads indicate cells on the tip of protrusions, while red arrows show straight cells that resemble the leaf elongated margin cells connecting to the protrusions. G and H, Numbers of hydathodes (G) and cell patches (H) of the sixth mature leaves in wild-type, *as2-1 rev-1*, and *kan1-11 kan2-5* plants. The number of the cell patches was examined on one side. $n = 10$, bars show SE. ** $P < 0.01$. I, Frequencies of the cell patches close to the hydathodes (within a range of 100 μm) in wild-type, *as2-1 rev-1*, and *kan1-11 kan2-5* leaves. Numbers above each column indicate total patches analyzed. J to L, Internal structures of the hydathode in wild-type Col-0 (J), and the protrusions in *as2-1 rev-1* (K) and *kan1-11 kan2-5* (L). ad, Adaxial leaf side; ab, abaxial leaf side; ve, vascular endings; et, epithem. Scale bars: 1 mm in A and D; 20 μm in B and E; 50 μm in C, F, and J to L.

YUC Genes Mediate Leaf Margin Development

Previous studies showed that the leaf margin produces auxin, which is essential for leaf blade outgrowth (Mattsson et al., 1999; Aloni et al., 2003; Zgurski et al., 2005). *YUC* genes function in local auxin biosynthesis, and removal of multiple *YUC* genes, such as *YUC1*, *2*, *4*, and *6*, resulted in plants with narrow leaves (Cheng et al., 2006, 2007). To determine whether *YUC* functions are required for leaf margin development, which may in turn affect blade outgrowth, we

analyzed leaf margins in *yuc* mutants. As *YUC1*, *2*, *4*, and *6* are functionally redundant (Cheng et al., 2006, 2007), we performed our phenotypic analysis using the *yuc1 yuc2 yuc4 yuc6* quadruple mutant. Compared with the wild type (Fig. 3A, left), the plants of *yuc1 yuc2 yuc4 yuc6* were smaller and showed a narrow-leaf phenotype (Fig. 3, A [right] and B). Interestingly, the leaf margin of *yuc1 yuc2 yuc4 yuc6* had only the elongated margin cells but lacked hydathodes (Fig. 3, B and C). In all cases, the same kind of cell patches observed in polarity-defective mutants was observed among the elongated margin cells in *yuc1 yuc2 yuc4 yuc6* (Fig. 3D), with an apparently increased number compared with that in wild-type leaves (Fig. 3E). These results suggest that *YUC*-mediated auxin biosynthesis is required for hydathode development. We also investigated the contribution of the four *YUC* genes to margin development and blade outgrowth, and found that *YUC1* and *YUC4* are likely to be the major contributors, while *YUC2* and *YUC6* act redundantly with *YUC1* and *YUC4* (Supplemental Fig. S2).

Different Expression Patterns of *YUC* Genes

To investigate the function of *YUC* genes in leaf margin development, we analyzed the expression patterns of *YUC1*, *2*, *4*, and *6* during leaf development by examining GUS staining of the first pair of rosette leaves in transgenic plants carrying the promoter-GUS fusions (Cheng et al., 2006, 2007). *YUC1* was expressed in the entire leaf primordium (Fig. 4, A and S), and the strongest GUS staining was found in the proximal part, which will ultimately develop into the petiole (Fig. 4, A and B). The GUS staining in the distal part of *pYUC1*::*GUS* leaves diminished gradually with primordium development (Fig. 4, B and C). *YUC1* staining was only detected in the proximal margin and the petiole of 8-DAG leaves (Fig. 4D). In older leaves, *YUC1* was expressed in the proximal end of the petiole (Fig. 4E). Interestingly, *YUC1* staining was also observed immediately distal to a hydathode (Fig. 4, E and F).

Expression of *YUC4* was not detected in young leaf primordia (Fig. 4G). During leaf development, the earliest *YUC4* expression was detected at the primordia on leaf tips in 3-DAG plants (Fig. 4H). As the leaf developed, GUS staining gradually intensified in hydathodes (Fig. 4, I–K, arrows). *YUC4* was also strongly expressed in vascular tissue connecting the leaf tip and hydathodes (Fig. 4, K and L). In regions near hydathodes, *YUC4* staining was found predominantly in the central layer cells (Fig. 4T). In the hydathode, the

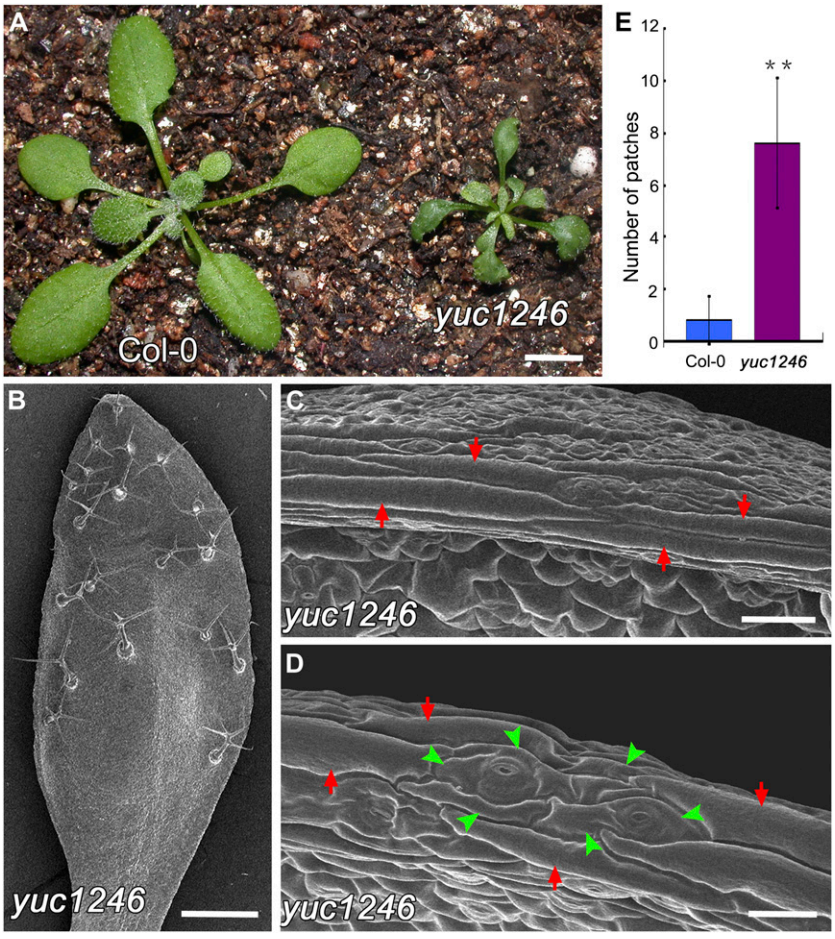

Figure 3. The *YUC* genes are required for leaf margin development. A, Compared with the 22-DAG wild-type Col-0 seedling (left), the *yuc1 yuc2 yuc4 yuc6* quadruple mutant (right) exhibits a small plant size. B, A sixth leaf of *yuc1 yuc2 yuc4 yuc6*. C and D, The *yuc1 yuc2 yuc4 yuc6* leaf margin contained only the margin cells (C, red arrows) and cell patches (D, green arrowheads) presenting among the margin cells (D, red arrows). E, The number of the cell patches was examined from one side of the sixth leaves in Col-0 and *yuc1 yuc2 yuc4 yuc6*. $n = 10$, bars show SE, and ** $P < 0.01$. *yuc1246*, *yuc1 yuc2 yuc4 yuc6*. Scale bars: 5 mm in A; 500 μm in B; 50 μm in C; 20 μm in D.

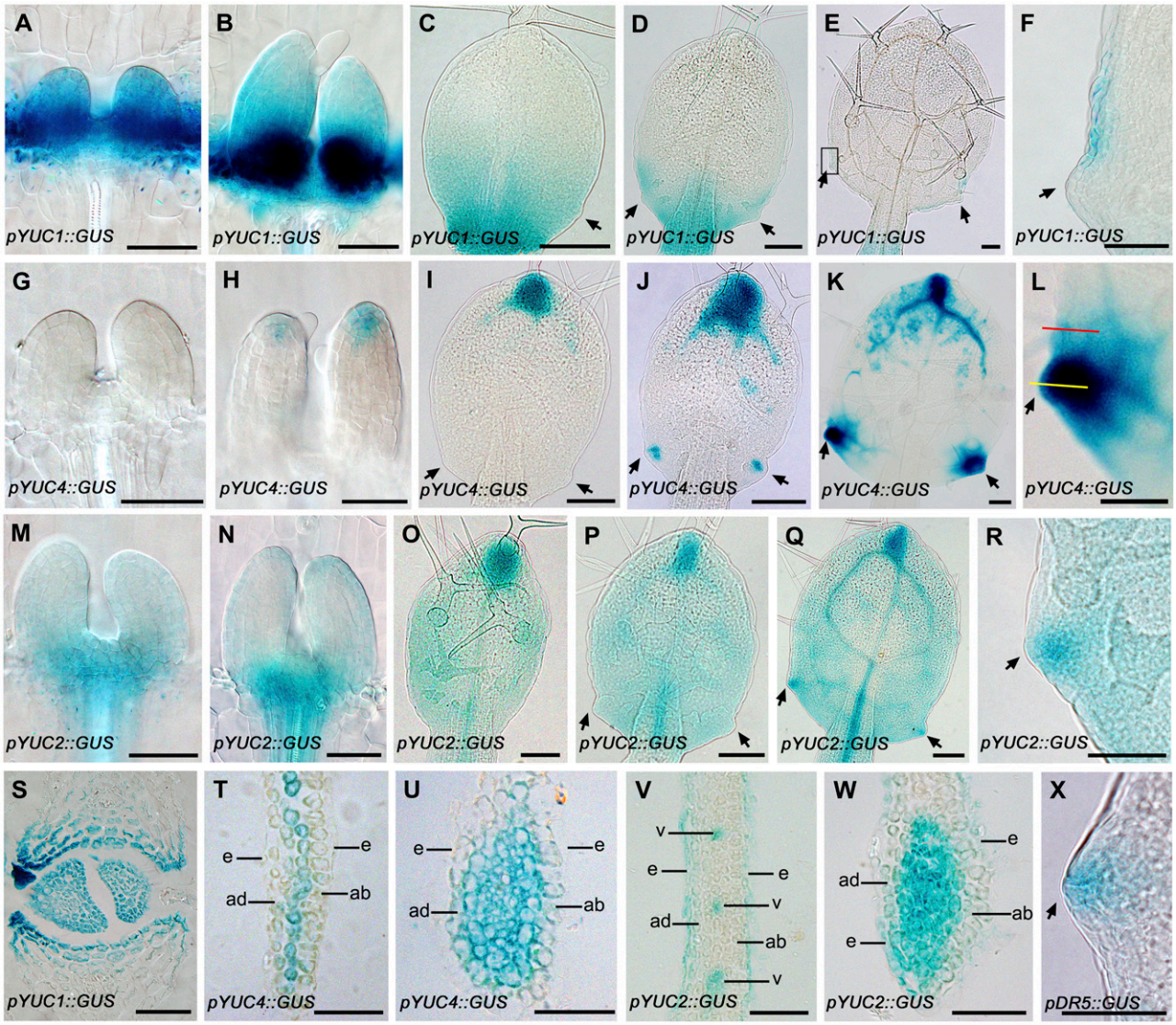

Figure 4. Spatially regulated *YUC* expression in the first pair of rosette leaves. A to E, GUS staining of leaf primordia or small leaves from the *pYUC1*::*GUS* transgenic plants including 2 DAG (A), 3 DAG (B), 6 DAG (C), 8 DAG (D), and 10 DAG (E). F, A hydathode boxed in E at higher magnification, showing that GUS staining was restricted in epidermal cells immediately distal to the hydathode. G to K, GUS staining of leaf primordia or small leaves from the *pYUC4*::*GUS* transgenic plants including 2 DAG (G), 3 DAG (H), 6 DAG (I), 7 DAG (J), and 10 DAG (K). L, Close-up of a hydathode in K, which was strongly stained. M to Q, GUS staining of leaf primordia or small leaves from the *pYUC2*::*GUS* transgenic plants including 2 DAG (M), 3 DAG (N), 5 DAG (O), 8 DAG (P), and 10 DAG (Q). R, A hydathode in Q at higher magnification. S to W, Transverse sections. *YUC1* was expressed in the entire leaf primordia (S). At a position indicated by a red line in L, *YUC4* staining was found in the central layer cells (T). In the hydathode, *YUC4* was highly expressed in the central part (U), indicated by a yellow line in L. *YUC2* was expressed in the epidermis, vasculature (V), and central layer cells in the hydathode (W). X, GUS staining of a transgenic wild-type plant carrying *pDR5*::*GUS* was concentrated in the tip of a hydathode. Arrows indicate hydathodes. ep, Epidermal cell layer; ad, adaxial mesophyll; ab, abaxial mesophyll; v, vasculature. Scale bars: 50 μm in A, B, F to H, L to N, and R to X; 100 μm in C to E, I to K, and O to Q.

number of cell layers was increased, and *YUC4* was preferentially expressed in the central-layer cells (Fig. 4U).

Weak *YUC2* staining was detected throughout the entire leaf primordium, whereas relatively strong GUS staining was observed in the meristem and the vascular tissue of hypocotyls (Fig. 4, M and N). However, during leaf development, the overall *YUC2* expression patterns were similar to those of *YUC4*, albeit with weaker GUS staining (Fig. 4, O–R). In addition, *YUC2* showed weak expression in the leaf epidermal cells and vascular tissue (Fig. 4V). Similar to *YUC4*, *YUC2* was also preferentially expressed in the central-layer cells of a hydathode (Fig. 4W).

We also analyzed expression of *YUC6*, but under our experimental conditions, we could not detect GUS staining in leaves of the *pYUC6*::*GUS* transgenic plants (data not shown). The different *YUC* expression patterns suggest that they may have specific functions in addition to their redundant ones, and the spatial expression in or surrounding hydathodes under the direction of leaf adaxial-abaxial juxtaposition implies that they might all contribute to hydathode development.

Ectopic Expression of *YUC* Genes in Leaves of *as2-1 rev-1* and *kan1-11 kan2-5*

To investigate whether the leaf adaxial-abaxial polarity affects *YUC* expression, we introduced *pYUC1*::*GUS*, *pYUC2*::*GUS*, and *pYUC4*::*GUS* into the *as2-1 rev-1* and *kan1-11 kan2-5* double mutants, and examined GUS staining in leaves. Because number of hydathodes was reduced in the leaves of these two double mutants (Fig. 2G) and *YUC4* was expressed in hydathodes (Fig. 4L), the number of GUS staining spots corresponding to hydathodes also decreased (Supplemental Fig. S1). The *YUC* expression patterns in later-appearing leaves of the wild type were similar to those in the first pair of leaves (Supplemental Fig. S3). Interestingly, expressions of *YUC1*, *YUC2*, and *YUC4* were associated with the protrusions on leaves of the two double mutants, similar to their expression patterns in hydathodes in wild-type leaves. In these two double mutants, *YUC1* staining was detected in epidermal cells distal to the protrusions (Fig. 5, A and E, arrows), and *YUC4* was expressed strongly in the tips of the finger-shaped protrusions (Fig. 5, B and F, arrows). Occasionally, small GUS staining spots were observed on leaf surfaces of both double mutants (Fig. 5, B and F, arrowheads), possibly reflecting emerging protrusions that were about to develop. The *YUC2* expression pattern in the protrusions was similar to that of *YUC4*, although the staining was weaker (Fig. 5, C and G, arrows).

To examine whether the ectopic *YUC* expression in the double mutant leaves causes abnormal auxin accumulation, we introduced the *pDR5*::*GUS* fusion (Ulmasov et al., 1997) into *as2-1 rev-1* and *kan1-11 kan2-5*. As a control, the DR5 staining in wild-type leaves primarily appeared in the leaf tip and hydathodes (Supplemental Fig. S3). However, GUS staining in the *as2-1 rev-1* or *kan1-11 kan2-5* leaves was also concentrated in the top portion of the protrusions (Fig. 5, D and H, arrows). This expression pattern was consistent with that in the hydathodes of wild-type leaves (Fig. 4X), which was located in a smaller region than that of *YUC4* expression (Fig. 4L). Together, our GUS staining data support the hypothesis that the ectopic protrusions on the double mutant leaves are hydathode-like structures, and the formation of these structures is closely related to auxin biology.

Leaf-Polarity-Mediated Margin Development Requires *YUC* Functions

To determine whether *YUC* genes contribute to leaf-polarity-mediated margin development, we constructed and analyzed the *as2-1 rev-1 yuc1 yuc2 yuc4* and *kan1-11 kan2-5 yuc1 yuc2 yuc4* pentuple mutants. Compared with the *as2-1 rev-1* double mutant (Fig. 6A, left), *as2-1 rev-1 yuc1 yuc2 yuc4*/+ plants were reduced in size (Supplemental Fig. S3), while *as2-1 rev-1 yuc1 yuc2 yuc4* plants were even smaller (Fig. 6A, right). Except for the first rosette leaves, the other leaves of *as2-1 rev-1 yuc1 yuc2 yuc4* were very small (Fig. 6, A and B), and the protrusions on the *as2-1 rev-1* double mutant leaves (Fig. 2A) were absent from both *as2-1 rev-1 yuc1 yuc2 yuc4*/+ (Fig. 6G) and *as2-1 rev-1 yuc1 yuc2 yuc4* plants (Fig. 6, C–F). The rosette leaves of one

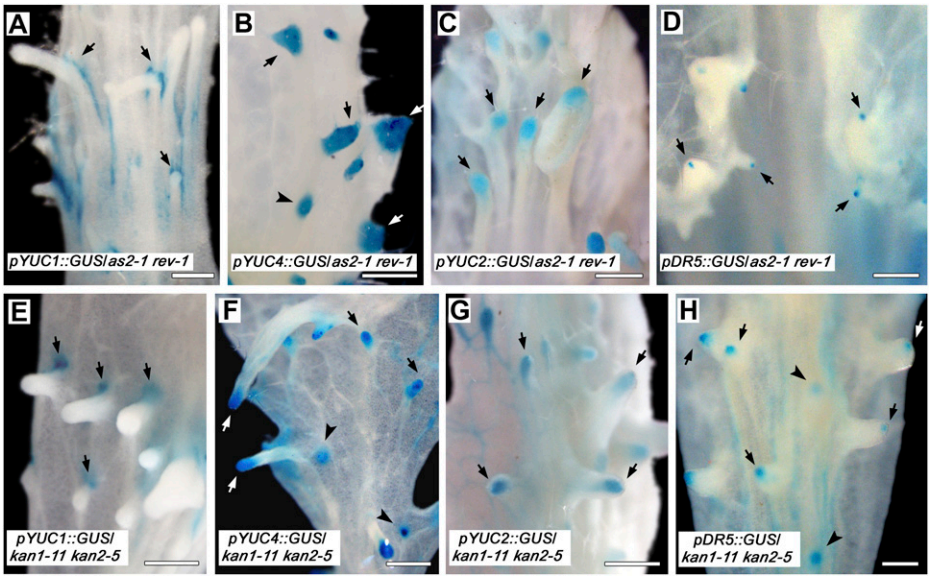

Figure 5. Ectopic expression of *YUC* genes in protrusions of *as2-1 rev-1* and *kan1-11 kan2-5* leaves. A to D, GUS staining of the 10th rosette leaves of *as2-1 rev-1* transgenic plants harboring the *pYUC1*::*GUS* (A), *pYUC4*::*GUS* (B), *pYUC2*::*GUS* (C), and *pDR5*::*GUS* (D) fusions. E to H, GUS staining of the sixth rosette leaves of the *kan1-11 kan2-5* transgenic plants carrying *pYUC1*::*GUS* (E), *pYUC4*::*GUS* (F), *pYUC2*::*GUS* (G), and *pDR5*::*GUS* (H) fusions. Arrows show the GUS accumulations associated with the protrusions, and arrowheads indicate the GUS staining representing hydathode-like structures that have not yet protruded. Scale bars: 200 μm in A, D, and H; 500 μm in B, C, E, F, and G.

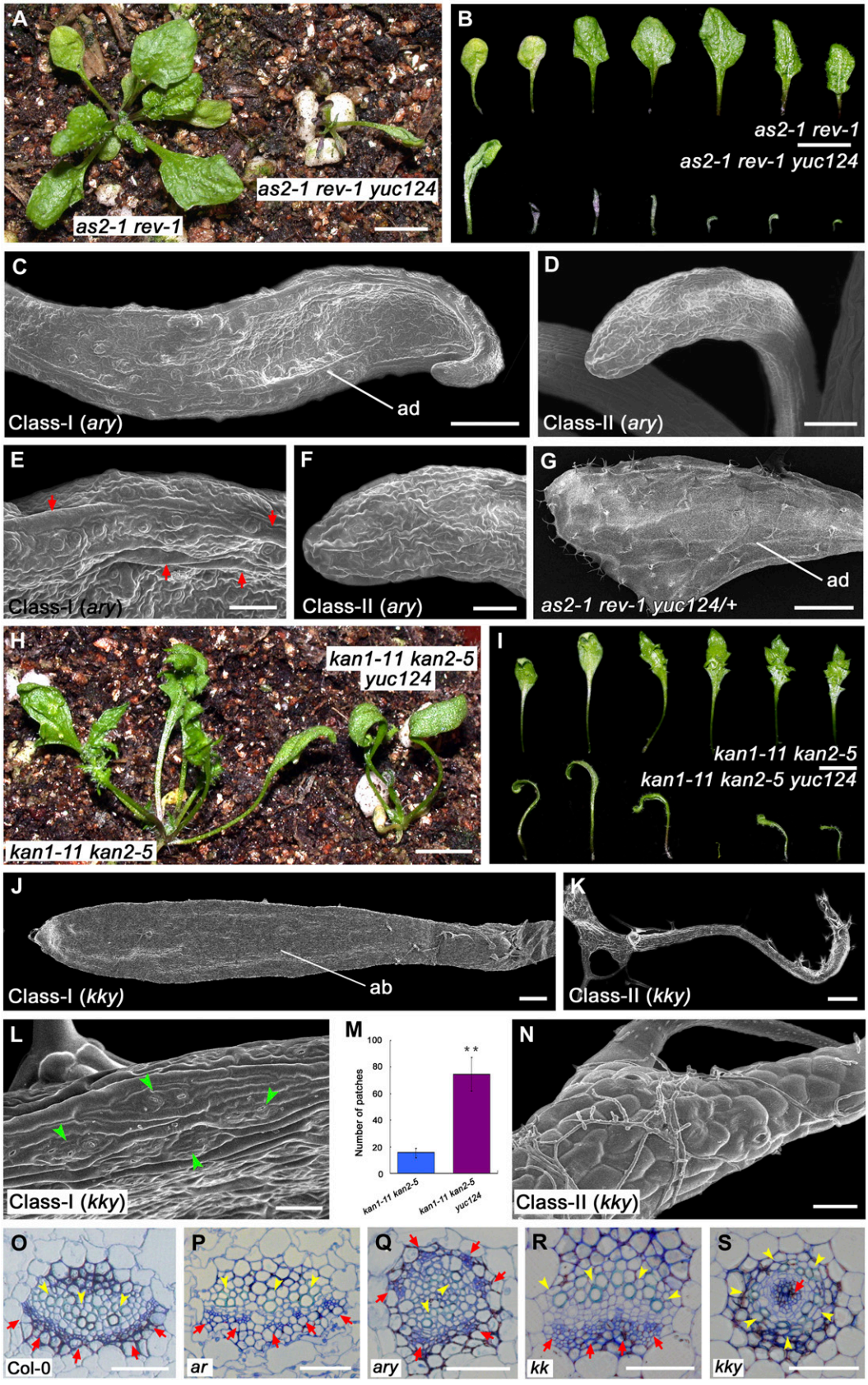

Figure 6. *YUC* genes are required for polarity-mediated margin development. A, The 27-DAG *as2-1 rev-1* (left) and *as2-1 rev-1*

as2-1 rev-1 yuc1 yuc2 yuc4 plant could be further classified into two classes based on their morphology. The class I leaves were narrow with the leaf margin curled upward (Fig. 6C); approximately the first four leaves belonged to this class. The margin formation of the class I leaves was severely defective with single elongated margin cells dispersed among the epidermal cells (Fig. 6E). The rest of the leaves of *as2-1 rev-1 yuc1 yuc2 yuc4* were class II leaves, which were filamentous structures lacking typical margin cells (Fig. 6, D and F). In addition, *as2-1 rev-1 yuc1 yuc2* and *as2-1 rev-1 yuc4 yuc6* plants did not show enhanced phenotypes of *as2-1 rev-1* (data not shown), while *as2-1 rev-1 yuc1 yuc2 yuc4* and *as2-1 rev-1 yuc1 yuc4 yuc6* showed more severe phenotypes, suggesting that *YUC1* and *YUC4* play major roles in polarity-mediated margin development (Supplemental Fig. S3).

In the wild type, the vasculature of the leaf midveins showed a pattern in which the xylem develops on the adaxial pole and phloem is located on the abaxial pole (Fig. 6O). This polar arrangement was also observed in mature *as2-1 rev-1* leaves (Fig. 6P). By contrast, a concentric ring of phloem surrounding xylem cells in the center was formed in the class II leaves of *as2-1 rev-1 yuc1 yuc2 yuc4* (Fig. 6Q), indicating the abaxialized leaf feature without any blade outgrowth.

The plant size of the *kan1-11 kan2-5 yuc1 yuc2 yuc4* pentuple mutant was also reduced (Fig. 6H), and its leaves were very narrow (Fig. 6, H and I). Compared with those in the *kan1-11 kan2-5* double mutant (Fig. 2D), the *kan1-11 kan2-5 yuc1 yuc2 yuc4* leaves lacked finger-shaped protrusions (Fig. 6J). Leaves of the *kan1-11 kan2-5 yuc1 yuc2 yuc4* mutant could also be divided into two classes. Most *kan1-11 kan2-5 yuc1 yuc2 yuc4* leaves were class I leaves, which exhibited a slightly expanded leaf blade (Fig. 6J), with margin cells interrupted by an increased number of cell patches on the leaf margin (Fig. 6, L and M), as compared with those in *kan1-11 kan2-5* (Fig. 2, E and H). In contrast, the class II leaves (only one to three leaves among the very-late-appearing ones) were very narrow structures with no margin cells (Fig. 6, K and N). Because the late-appearing *yuc1 yuc2 yuc4 yuc6* leaves were narrower than the early ones (Fig. 3A), when this mutant was combined with *kan1 kan2*, which also produces narrow leaves, the late-appearing leaves became even narrower. It is possible that the extremely narrowed leaves may easily form filamentous structures lacking the leaf margin. We also analyzed the xylem and phloem arrangement of the class II leaves of *kan1-11 kan2-5 yuc1 yuc2 yuc4* plants. Compared with that in *kan1-11 kan2-5* (Fig. 6R), the phloem of the leaf midvein in *kan1-11 kan2-5 yuc1 yuc2 yuc4* was surrounded by the xylem (Fig. 6S), indicating that the pentuple mutant leaves are adaxialized with no blade outgrowth. Together, these data indicate that *YUC* functions are required for the formation of protrusions on leaf surfaces of the polarity-defective double mutants, and that auxin biosynthesis is essential for leaf-polarity-directed margin development.

Polar Auxin Transport Is Involved in Leaf Margin Formation and Blade Outgrowth

Previous studies showed that treatment with auxin transport inhibitors results in altered leaf vascular patterns and smaller leaves in Arabidopsis (Mattsson et al., 1999). Auxin transport is also required for the formation of serrations on the leaf margin (Aloni et al., 2003; Hay et al., 2006). To investigate whether hydathode formation also requires auxin transport, we examined leaf margin development after treatment with an auxin transport inhibitor *N*-(1-naphtyl) phtalamic acid (NPA). Our data showed that treatment with 1 μM NPA reduced the size of wild-type seedlings and leaves, and treatment with 5 μM NPA caused even greater reductions (Fig. 7, A, C, and E). In addition, treatment with 1 μM NPA significantly decreased the number of hydathodes (Fig. 7S), and treatment with 5 μM NPA resulted in a complete lack of hydathodes (data not shown). Compared with the mock-treated wild type (Fig. 7B), treatment with 1 μM NPA also resulted in the disordered arrangement of margin cells (Fig. 7D, arrows), while many parts of the leaf margin lacked margin cells when treated with 5 μM NPA (Fig. 7F).

Similarly, treatment with increased NPA concentrations resulted in decreased plant size of *as2-1 rev-1*

Figure 6. (*Continued.*)
yuc1 yuc2 yuc4 (right) seedlings. B, Leaves from the 27-DAG *as2-1 rev-1* (top) and *as2-1 rev-1 yuc1 yuc2 yuc4* (bottom) seedlings. C to F, *as2-1 rev-1 yuc1 yuc2 yuc4* leaves, which are divided into two classes, class I (C) and class II (D) leaves. Leaf margin of the class I leaves contains disrupted margin cells (red arrows; E), while the class II leaves exhibits a complete loss of margin cells (F). G, Adaxial surface of a 10th leaf in *as2-1 rev-1 yuc1 yuc2 yuc4*/+, showing that the finger-like structures were absent. H, The 27-DAG *kan1-11 kan2-5* (left) and *kan1-11 kan2-5 yuc1 yuc2 yuc4* (right) seedlings. I, Leaves from the 27-DAG *kan1-11 kan2-5* (top) and *kan1-11 kan2-5 yuc1 yuc2 yuc4* (bottom) seedlings. J and K, The class I (J) and the class II (K) *kan1-11 kan2-5 yuc1 yuc2 yuc4* leaves. L, Leaf margin of the class I *kan1-11 kan2-5 yuc1 yuc2 yuc4* leaves has the disrupted margin cells with multiple ectopic patches (green arrowheads). M, The number of the cell patches from one side of the sixth leaves in *kan1-11 kan2-5* and *kan1-11 kan2-5 yuc1 yuc2 yuc4*. $n = 10$, bars show SE, and ** $P < 0.01$. N, Class II *kan1-11 kan2-5 yuc1 yuc2 yuc4* leaves contain no margin cells. O to S, Transverse sections of the midvein of mature leaves in Col-0 (O), *as2-1 rev-1* (P), *as2-1 rev-1 yuc1 yuc2 yuc4* (class II; Q), *kan1-11 kan2-5* (R), and *kan1-11 kan2-5 yuc1 yuc2 yuc4* (class II; S). Arrowheads indicate xylem, and arrows show phloem. ad, Adaxial leaf side; ab, abaxial leaf side; *yuc124*, *yuc1 yuc2 yuc4*; *yuc124*/+, *yuc1 yuc2 yuc4*/+; *ar*, *as2-1 rev-1*; *ary*, *as2-1 rev-1 yuc1 yuc2 yuc4*; *kk*, *kan1-11 kan2-5*; *kky*, *kan1-11 kan2-5 yuc yuc1 yuc2 yuc4*. Scale bars: 5 mm in A, B, H, and I; 200 μm in C, J, and K; 100 μm in D; 50 μm in E, F, L, and O to S; 1 mm in G; 20 μm in N.

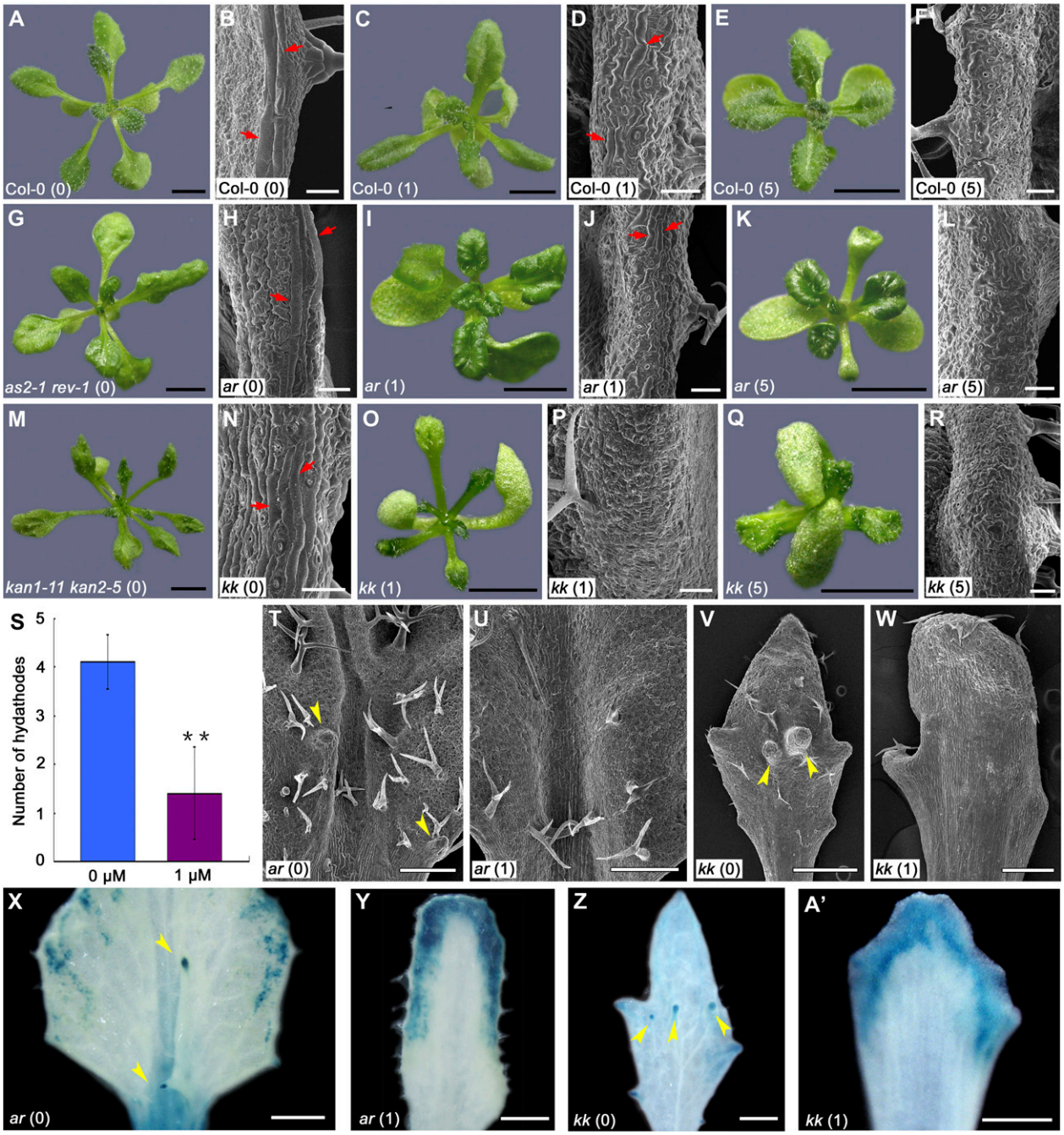

Figure 7. Polar auxin transport is required for leaf margin development and blade outgrowth. Plants were grown on media containing 0.5× Murashige and Skoog salts with different concentrations of NPA. A, B, G, H, M, and N, The 18-DAG Col-0 (A and B), *as2-1 rev-1* (G and H), and *kan1-11 kan2-5* (M and N) seedlings, whose leaf margins of the fourth leaf were examined by SEM. C, D, I, J, O, and P, The 18-DAG Col-0 (C and D), *as2-1 rev-1* (I and J), and *kan1-11 kan2-5* (O and P) seedlings grown on media containing 1 μM NPA; leaf margins of the fourth leaf were examined by SEM. E, F, K, L, Q, and R, 18-DAG Col-0 (E and F), *as2-1 rev-1* (K and L), and *kan1-11 kan2-5* (Q and R) seedlings grown on media containing 5 μM NPA, whose leaf margins of the fourth leaf were examined by SEM. S, Numbers of hydathodes of the fourth leaves of Col-0 grown on media with or without 1 μM NPA. $n = 10$, and bars show SE. ** $P < 0.01$. T and U, The adaxial surface of the ninth leaves from *as2-1 rev-1* seedlings grown on media with (U) or without (T) 1 μM NPA. V and W, The abaxial surface of the fourth leaves in *kan1-11 kan2-5* seedlings grown with (W) or without (V) 1 μM NPA. X and Y, Adaxial surface of the ninth leaves from *pYUC4*::*GUS*/*as2-1 rev-1* seedlings grown on media with (Y) or without (X) 1 μM NPA. Z and A', Abaxial surface of the fourth leaves in *pYUC4*::*GUS*/*kan1-11 kan2-5* seedlings grown with (A') or without (Z) 1 μM NPA. Red arrows indicate margin cells, and yellow arrowheads show protrusions. *ar*, *as2*-1 *rev-1*; *kk*, *kan1-11 kan2-5*. The numbers in brackets indicate NPA concentrations (μM). Scale bars: 3 mm in A, C, E, G, I, K, M, O, and Q; 50 μm in B, D, F, H, J, L, N, P, and R; 200 μm in T, U, W, and Y; 500 μm in V, X, Z, and A'.

(Fig. 7, G, I, and K) and *kan1-11 kan2-5* (Fig. 7, M, O, and Q) double mutants. Compared with the mock-treated *as2-1 rev-1* (Fig. 7H) and *kan1-11 kan2-5* (Fig. 7N), treatment of the double mutants with NPA led to leaves with very few (Fig. 7J, arrows) or no margin cells (Fig. 7, L, P, and R). It is possible that leaf margin development is already compromised in the polarity mutant backgrounds, making these mutants more sensitive than wild-type plants to NPA. We also analyzed the finger-shaped protrusions on *as2-1 rev-1* and *kan1-11 kan2-5* leaves, and found that these structures were completely absent after treatment with 1 μM NPA (Fig. 7, T–W). This result indicates that in addition to auxin biosynthesis, polar auxin transport is also required for development of protrusions. These results are also consistent with the previous model that leaf polarity regulators act via regulating auxin flow (Izhaki and Bowman, 2007; Ilegems et al., 2010).

To investigate whether genes for auxin biosynthesis are regulated by auxin polar transport during blade outgrowth, we analyzed *YUC4* expression by examining the *pYUC4*::*GUS* fusion in *as2-1 rev-1* and *kan1-11 kan2-5* double mutants, with or without NPA treatment. *YUC4* was expressed in the leaf protrusions of the mock-treated *as2-1 rev-1* and *kan1-11 kan2-5* (Fig. 7, X and Z), whereas the *YUC4* expression pattern was altered in leaves of both the double mutants when they were treated with 1 μM NPA (Fig. 7, Y and A′). In particular, in both of the double mutants, we did not observe the small GUS-staining spots on leaf surfaces (Fig. 5, B and F, arrowheads) that reflected emerging protrusions. These results indicate that *YUC* expression during leaf development also relies on polar auxin transport, and suggest that the transport-mediated auxin gradient is important for leaf margin formation and blade outgrowth.

To provide additional evidence for the importance of an auxin gradient in leaf margin formation, we introduced the *35S*::*YUC1* fusion into wild-type Col-0 and *kan1-11 kan2-5* plants, because the ubiquitously expressed *YUC1* may disturb the endogenous auxin gradient. The *35S*::*YUC1* transgenic plants displayed phenotypes with varying degrees of severity, and could be grouped into three classes. Class I plants showed almost wild-type or *kan1-11 kan2-5* phenotypes (Fig. 8, B and F), while class II (Fig. 8, C and G) and class III (Fig. 8, D and H) plants displayed moderate and strong auxin overproduction phenotypes, respectively, as reported previously (Cheng et al., 2006). In particular, the class III plants became very small in both wild-type (inset in Fig. 8A) and *kan1-11 kan2-5* mutant (inset in Fig. 8E) backgrounds. Quantitative real-time reverse transcription (qRT)-PCR revealed that the severity of the phenotypes of the transgenic plants was correlated with the levels of *YUC1* transcripts (Fig. 8I). More detailed analyses showed that both class III *35S*::*YUC1*/Col-0 and *35S*::*YUC1*/*kan1-11 kan2-5* plants contained significantly less hydathodes than the wild type (Fig. 8J). The number and the size of the abaxial protrusions of the class III *35S*::*YUC1*/*kan1-11 kan2-5* plants were also reduced compared with those of *kan1-11 kan2-5* (Fig. 8, K–N). These results further support the model that leaf margin formation and blade outgrowth require an endogenous auxin gradient.

DISCUSSION

It was proposed that finger-shaped protrusions were caused by the ectopic juxtaposition of the leaf adaxial and abaxial domains in the *as2-1 rev-1* and *kan1-11 kan2-5* mutants (Eshed et al., 2004; Fu et al., 2007). In this work, our data suggest that *YUC* genes might respond to the newly formed juxtaposition in the leaves of these two double mutants, leading to the induction of finger-shaped protrusions. This process in the double mutants is consistent with hydathode specification in leaf margins, where the adaxial-abaxial juxtaposition is formed.

A typical hydathode has specific epidermal cells, an internal structure, and expressions of *DR5* and *YUC*. We obtained several lines of evidence indicating that the finger-shaped protrusions on the leaf surfaces of *as2 rev* and *kan1 kan2* are hydathode-like structures: (1) the cell morphology of protrusions is similar to that of hydathodes, both comprising irregularly shaped cells mixed with stomata in their epidermis; (2) the hydathodes and the top part of the protrusions both connect to long straight cells, either in the margin or on the adaxial and abaxial leaf surfaces; (3) the protrusions contain internal structures similar to those in hydathodes; (4) expression patterns of different *YUC* genes and the *pDR5*::*GUS* fusion are similar in hydathodes and protrusions; and (5) formation of both hydathodes and protrusions is dependent on *YUC* activity and polar transport of auxin, and this was observed even in leaves of transgenic plants ectopically expressing the leaf polarity gene *AS2* (Supplemental Fig. S4). Identification of a marker gene that is specifically expressed in the hydathode will be a key step for the final conclusion that hydathodes and protrusions are the same tissues. Because the leaf margin harboring hydathodes is in the region of convergence of the adaxial and abaxial leaf domains, it is possible that hydathode formation requires normal establishment of leaf adaxial-abaxial polarity.

The *as2 rev* and *kan1 kan2* double mutants appear to be useful tools to investigate leaf margin development. Although these two double mutants have adaxialized (*kan1 kan2*) or abaxialized (*as2 rev*) leaves, they have a similarly defective leaf margin with a reduced number of hydathodes but an increased number of cell patches. Therefore, their leaf-polarity defects, regardless of adaxial or abaxial abnormalities, share a common mechanism that causes a similar leaf margin defect. A defective margin is possibly the main reason for inhibition of blade outgrowth in both adaxialized and abaxialized leaf polarity mutants, and genetic pathways that respond to adaxial-abaxial leaf polarity

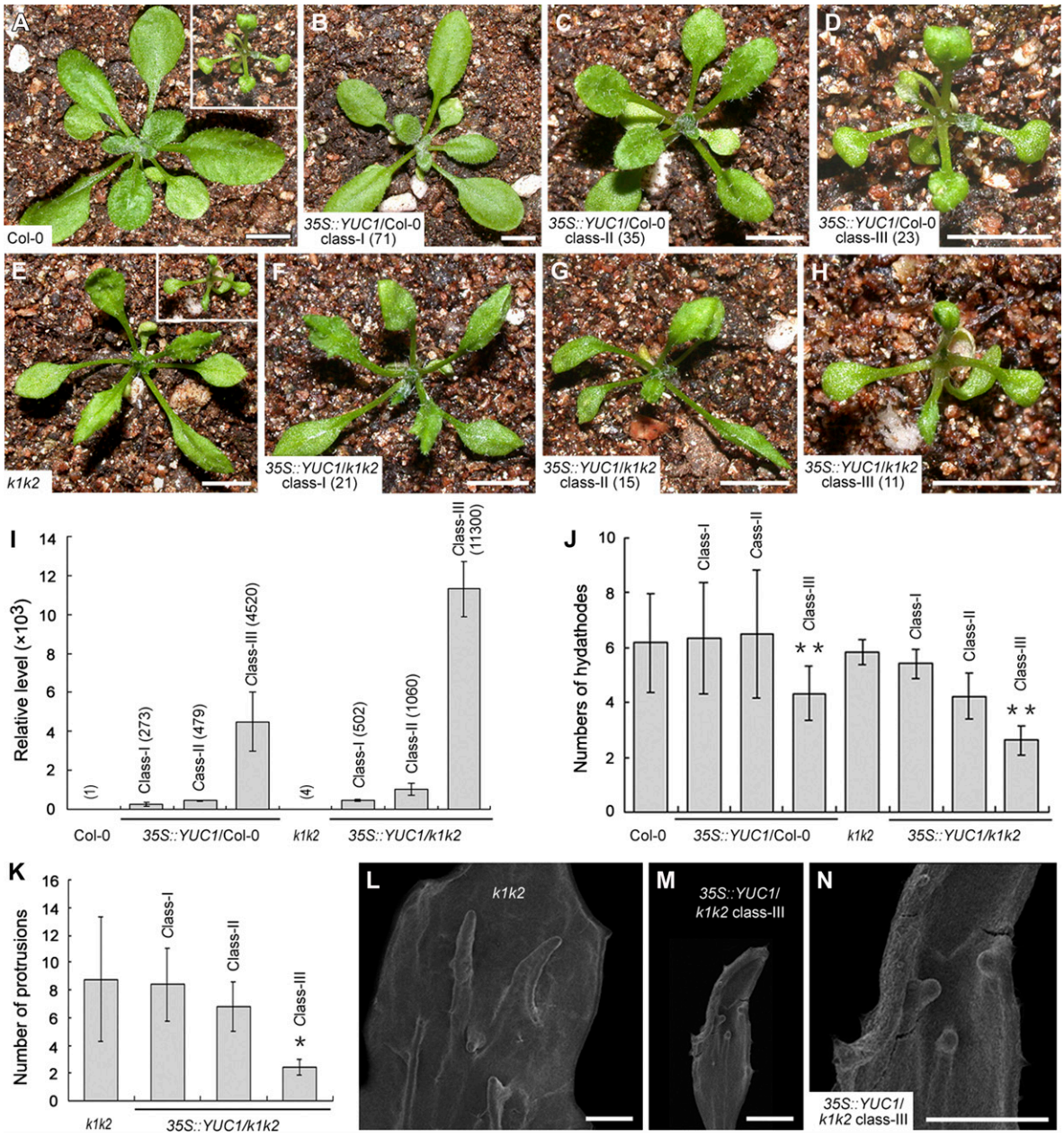

Figure 8. Characterization of *35S::YUC1*/Col-0 and *35S::YUC1*/*kan1-11 kan2-5* transgenic plants. Plants of 20 DAG were used in analyses (A–H). A to D, A wild-type Col-0 plant (A), and a class I (B), II (C), and III (D) *35S::YUC1*/Col-0 plant. E to H, A *kan1-11 kan2-5* plant (E), and a class I (F), II (G), and III (H) *35S::YUC1*/*kan1-11 kan2-5* plant. *35S::YUC1* was introduced into plants by *Agrobacterium*-mediated transformation. Numbers in brackets of B to D and F to H indicate total independent transgenic plants obtained from one transformation experiment. I, qRT-PCR analyses show that *YUC1* transcript levels were increased in transgenic plants, compared with those in Col-0 and *kan1-11 kan2-5* plants, and phenotypic severity of the transgenic plants correlates to levels of the elevated *YUC1* transcripts. The qRT-PCR results were normalized to that of *ACTIN*. Numbers in brackets indicate folds of elevation, and bars indicate SE. J, Analysis of leaf hydathodes of transgenic plants that are in the Col-0 and *kan1-11 kan2-5* backgrounds. The sixth leaves were used, and bars indicate SE. ** $P < 0.01$, $n = 6$. Note that the hydathode number between Col-0 and *kan1-11 kan2-5* is close, probably because the first 7 d of growth of these plants was on plates. K, The number of the abaxial protrusions on the sixth leaves of the class III *35S::YUC1*/*kan1-11 kan2-5* transgenic plants was reduced compared with those of *kan1-11 kan2-5*. Bars indicate SE. * $P < 0.05$, $n = 5$. L and M, SEM analysis of class III *35S::YUC1*/*kan1-11 kan2-5* leaves. Compared with the size of abaxial protrusions on the sixth *kan1-11 kan2-5* leaves (L), that of the *35S::YUC1*/*kan1-11 kan2-5* protrusions was reduced (M). N, Close-up of the protrusions in M. *k1k2*, *kan1-11 kan2-5*. Scale bars: 5 mm in A to H; 1 mm in L to N.

must be commonly affected in leaf margin development in both double mutants.

In this work, we found that expressions of *YUC1*, *YUC2*, and *YUC4* are associated with hydathodes and protrusions of polarity-defective double mutants, indicating that functions of these *YUC* genes are involved in at least one pathway that responds to the adaxial-abaxial polarity of the leaf. In addition, these *YUC* genes are required for leaf margin development through promoting hydathode growth, as leaf margins of the *yuc1 yuc2 yuc4 yuc6* quadruple mutants lacked hydathodes and the polarity double mutants had fewer hydathodes than the wild type. Finally, *yuc1 yuc2 yuc4 yuc6* produced narrow leaves, also seen in the polarity double mutants, indicating that the *YUC* functions are required for blade outgrowth. Therefore, expressions of these *YUC* genes in response to the adaxial-abaxial juxtaposition at correct locations might be one of the key steps in margin development and blade outgrowth. It would be very interesting to determine whether *YUC1*, *YUC2*, and *YUC4* are directly regulated by leaf polarity genes. Alternatively, because both leaf polarity and auxin biosynthesis genes studied in this work is likely redundant with some others, respectively, it is also possible that the two pathways may converge in leaf margin formation.

YUCs are expressed in or near hydathodes, implying that auxin concentrations may be relatively high around the position of hydathode initiation. However, our data show a possibility that the surrounding auxin must be further concentrated by an auxin transport mechanism. Treatment with a low concentration of the auxin transport inhibitor NPA not only affected normal margin formation in the wild-type leaves, but also severely affected *YUC4* expression patterns and completely blocked development of finger-shaped protrusions on leaf surfaces of both *as2 rev* and *kan1 kan2*. Active transport of auxin can achieve the auxin maxima required for patterning of different plant tissues or organs (Heisler et al., 2005; Petrásek et al., 2006; Scarpella et al., 2006). It is possible that hydathode formation may also require an auxin maximum in the leaf margin. In addition, ectopic overexpression of *YUC* genes may weaken the auxin gradient between the hydathode and its surrounding tissues, and thus severely affected the margin formation and blade outgrowth of leaves in the *35S*::*YUC1* plants.

It is possible that patches associated with elongated leaf margin cells represent the epidermis on the top portion of hydathodes, because the shapes of the cells on the tops of hydathodes and patches are very similar, and both contain stomata. However, expression of the hydathode marker *pYUC1/2/4*::*GUS* or *pDR5*::*GUS* was not detected in the cells in these patches (data not shown). Using a leaf margin marker line YJ158 (Eshed et al., 2004), we found that the elongating margin cells, the hydathode, and the patch cells all showed GUS staining in young leaves, whereas GUS staining weakened in fully differentiated hydathodes (Supplemental Fig. S5). These data suggest that patches are aborted hydathodes that lack the internal structures and are unable to protrude further. The main differences between the wild type and polarity or *yuc* multiple mutants were the number of patches and their distribution along the leaf margins. It is possible that the initiation of hydathodes requires an auxin maximum, whereas patch formation only requires dispersed or low concentrations of auxin. During hydathode formation, auxin leakage from areas of high auxin concentration in the wild-type leaf margin might result in patch formation. This could explain why most patches are close to a hydathode in the wild-type leaf margin, whereas the leaf margin contains dispersed patches but no hydathodes in the *yuc1 yuc2 yuc4 yuc6* mutant. Because disrupted leaf polarity alters *YUC* expression patterns, the abnormal auxin biosynthesis also resulted in more cell patches and less hydathodes in the leaf-polarity-defective mutants.

Auxin has long been known to play different roles in the leaf margin. Recent studies have implicated auxin distribution as a patterning mechanism for compound leaves, and blocking auxin transport results in leaf simplification (Avasarala et al., 1996; Reinhardt et al., 2000; DeMason and Chawla, 2004; Barkoulas et al., 2008). Arabidopsis and *Cardamine hirsuta* are distantly related species, but have simple and dissected leaves with an individual leaflet, respectively. It was reported that lateral leaflet formation in *C. hirsuta* requires establishment of growth foci that develop after leaf initiation. The growth foci are recruited at the leaf margin in response to the auxin maxima (Barkoulas et al., 2008). This situation is comparable to development of serrations in some Arabidopsis leaves (Hay et al., 2006) and of hydathodes in this work. In all these cases, auxin maxima are established in these special leaf-margin-containing tissues: i.e. the growth foci, the serration tips, and the hydathodes. Therefore, the formation of these tissues may follow a common mechanism. With strong auxin maxima and perhaps some other gene functions, the growth foci would develop into leaflets. Without some of these conditions, leaf margins might only produce less-pronounced serrations or, with even weaker signals, hydathodes. Because of the similarity in cellular patterns between hydathodes and leaf margin cell patches, we further propose that when marginal auxin maxima are lacking, such as in the leaf-polarity-defective mutants or in the multiple *yuc* mutants, instead of hydathodes the more dispersed cell patches develop in the leaf margin.

MATERIALS AND METHODS

Plant Materials and Growth Conditions

Seeds of *as2-1* (ER, CS3117) and *rev-1* (Nossen, CS3826) were obtained from the Arabidopsis Biological Resource Center. Double mutant *as2-1 rev-1* was constructed by crossing *rev-1* to *as2-1*, and in the F2 segregating population,

the plants with phenotypes similar to the previously reported *as2-101 rev-6* double mutant (Fu et al., 2007) were considered to be the *as2-1 rev-1* double mutant. *as2-1 rev-1* was backcrossed to Col-0 twice, and the *as2-1 rev-1* phenotypes were consistent in the F2 progeny. Seeds of *kan1-11 kan2-5/+* (Col-0), enhancer trap marker line YJ158, and transgenic plants carrying *pYUC1*::*GUS*, *pYUC2*::*GUS*, *pYUC4*::*GUS*, *pYUC6*::*GUS*, and *pDR5*::*GUS* were kindly provided by R.S. Poethig (Wu et al., 2008), Y. Eshed (Eshed et al., 2004), Y. Zhao (Zhao et al., 2001; Cheng et al., 2006), and T.J. Guilfoyle (Ulmasov et al., 1997), respectively. Plant growth in soil and on media was according to our previous conditions (Chen et al., 2000; Qi et al., 2004).

Construction of Pentuple Mutants

Plants from a segregating population containing multiple heterozygous *yuc1 yuc2 yuc4 yuc6* were first genotyped as described (Cheng et al., 2006), and a plant carrying *yuc1 yuc2/+ yuc4/+ yuc6* was identified. For construction of the *as2-1 rev-1 yuc1 yuc2 yuc4* pentuple mutant, *yuc1 yuc2/+ yuc4/+ yuc6* was crossed to *as2-1 rev-1*. In F2 progeny, plants with *as2-1 rev-1* phenotypes were genotyped for the presence of *yuc1*, *yuc2*, *yuc4*, and *yuc6*, and the *as2-1 rev-1 yuc1 yuc2/+ yuc4/+* or *as2-1 rev-1 yuc1 yuc2 yuc4/+* plants were harvested for further segregation. Plants with similar novel phenotypes appeared among both F3 progeny, and these phenotypically novel plants were subsequently genotyped to show that they carried *as2-1 rev-1 yuc1 yuc2 yuc4* mutations. For construction of the *kan1-11 kan2-5 yuc1 yuc2 yuc4* pentuple mutant, the *yuc1 yuc2/+ yuc4/+ yuc6* plants were crossed to *kan1-11 kan2-5/+*, as homozygous *kan1-11 kan2-5* is sterile. In F2 progeny, plants with *kan1-11 kan2-5/+* phenotypes were genotyped, and plants with the *kan1-11 kan2-5/+ yuc1 yuc2/+ yuc4/+* and *kan1-11 kan2-5/+ yuc1 yuc2 yuc4/+* mutations were isolated. The mutant seeds were harvested for further segregation analysis. In the F3 progeny, plants with novel phenotypes were genotyped to obtain the *kan1-11 kan2-5 yuc1 yuc2 yuc4* pentuple mutants.

GUS Staining and Microscopy

The histochemical detection of GUS activity was according to our previous methods (Li et al., 2005), with a staining incubation time of 6 h. The stained tissues were cleared as previously described when needed (Lee et al., 2009), and the microscopic images were obtained using a differential interference contrast microscope. Preparing plant material sections was as previously described (Xu and Shen, 2008). The SEM analysis was performed according to the previously described methods (Chen et al., 2000). The red fluorescent dye *N*-(3-triethylammoniumpropyl)-4-(*p*-diethylaminophenylhexatrienyl)-pyridinium 2Br (FM4-64; 5 μg/mL) that intercalates into the plasma membrane was imaged at 543 nm excitation to visualize epidermal cells of leaf primordia.

qRT-PCR

Total RNA was extracted from the 20-DAG leaves of independent transgenic plants. qRT-PCR was performed according to our previous method (Li et al., 2005). Primers for detection of *ACTIN* transcripts were 5′-TGGCATCA (T/C)ACTTTCTACAA-3′ and 5′-CCACCACT(G/A/T)AGCACAATGTT-3′, and those for *YUC1* transcripts were 5′-GAAGCGAGATCCATACTTC-3′ and 5′-GTATCTCCCTTGGCAACA-3′.

Sequence data used in this study can be found in the Arabidopsis Genome Initiative database under the following accession numbers: YUC1 (At4g32540), AS2 (At1g65620), and FIL (At2g45190).

Supplemental Data

The following materials are available in the online version of this article.

Supplemental Figure S1. The number of hydathodes is reduced in the *as2-1 rev-1* and *kan1-11 kan2-5* double mutants.

Supplemental Figure S2. Contributions of *YUC* genes in leaf margin development and leaf adaxial-abaxial polarity establishment.

Supplemental Figure S3. Expression patterns of *pYUC1*::*GUS*, *pYUC2*::*GUS*, *pYUC4*::*GUS*, and *pDR5*::*GUS* in later-appearing leaves, and phenotypes of *as2-1 rev-1*, *as2-1 rev-1 yuc1 yuc2 yuc4/+*, and *as2-1 rev-1 yuc1 yuc4 yuc6*.

Supplemental Figure S4. Formation of leaf protrusions in the *pFIL*::*AS2* transgenic plants is dependent on *YUC* activity.

Supplemental Figure S5. GUS staining of YJ158 in the wild type.

ACKNOWLEDGMENTS

We thank X. Gao for SEM; R.S. Poethig for seeds of *kan1-11 kan2-5/+*; Y. Zhao for seeds of *yuc1 yuc2/+ yuc4/+ yuc6* and *pYUC1*::*GUS*, *pYUC2*::*GUS*, *pYUC4*::*GUS*, and *pYUC6*::*GUS* transgenic plants; T.J. Guilfoyle and Y. Eshed for seeds of *pDR5*::*GUS* and YJ158 marker lines, respectively; and the Arabidopsis Biological Resource Center for seeds of *as2-1* and *rev-1*.

Received August 29, 2011; accepted October 12, 2011; published October 14, 2011.

LITERATURE CITED

Aloni R, Schwalm K, Langhans M, Ullrich CI (2003) Gradual shifts in sites of free-auxin production during leaf-primordium development and their role in vascular differentiation and leaf morphogenesis in *Arabidopsis*. Planta **216:** 841–853

Avasarala S, Yang J, Caruso JL (1996) Production of phenocopies of the lanceolate mutant in tomato using polar auxin transport inhibitors. J Exp Bot **47:** 709–712

Barkoulas M, Hay A, Kougioumoutzi E, Tsiantis M (2008) A developmental framework for dissected leaf formation in the *Arabidopsis* relative *Cardamine hirsuta*. Nat Genet **40:** 1136–1141

Benjamins R, Scheres B (2008) Auxin: the looping star in plant development. Annu Rev Plant Biol **59:** 443–465

Bowman JL, Floyd SK (2008) Patterning and polarity in seed plant shoots. Annu Rev Plant Biol **59:** 67–88

Chen C, Wang S, Huang H (2000) *LEUNIG* has multiple functions in gynoecium development in *Arabidopsis*. Genesis **26:** 42–54

Cheng Y, Dai X, Zhao Y (2006) Auxin biosynthesis by the YUCCA flavin monooxygenases controls the formation of floral organs and vascular tissues in *Arabidopsis*. Genes Dev **20:** 1790–1799

Cheng Y, Dai X, Zhao Y (2007) Auxin synthesized by the YUCCA flavin monooxygenases is essential for embryogenesis and leaf formation in *Arabidopsis*. Plant Cell **19:** 2430–2439

DeMason DA, Chawla R (2004) Roles for auxin during morphogenesis of the compound leaves of pea (*Pisum sativum*). Planta **218:** 435–448

Donnelly PM, Bonetta D, Tsukaya H, Dengler RE, Dengler NG (1999) Cell cycling and cell enlargement in developing leaves of *Arabidopsis*. Dev Biol **215:** 407–419

Emery JF, Floyd SK, Alvarez J, Eshed Y, Hawker NP, Izhaki A, Baum SF, Bowman JL (2003) Radial patterning of *Arabidopsis* shoots by class III HD-ZIP and KANADI genes. Curr Biol **13:** 1768–1774

Eshed Y, Baum SF, Perea JV, Bowman JL (2001) Establishment of polarity in lateral organs of plants. Curr Biol **11:** 1251–1260

Eshed Y, Izhaki A, Baum SF, Floyd SK, Bowman JL (2004) Asymmetric leaf development and blade expansion in *Arabidopsis* are mediated by KANADI and YABBY activities. Development **131:** 2997–3006

Fu Y, Xu L, Xu B, Yang L, Ling Q, Wang H, Huang H (2007) Genetic interactions between leaf polarity-controlling genes and *ASYMMETRIC LEAVES1* and *2* in *Arabidopsis* leaf patterning. Plant Cell Physiol **48:** 724–735

Hay A, Barkoulas M, Tsiantis M (2006) ASYMMETRIC LEAVES1 and auxin activities converge to repress *BREVIPEDICELLUS* expression and promote leaf development in *Arabidopsis*. Development **133:** 3955–3961

Heisler MG, Ohno C, Das P, Sieber P, Reddy GV, Long JA, Meyerowitz EM (2005) Patterns of auxin transport and gene expression during primordium development revealed by live imaging of the *Arabidopsis* inflorescence meristem. Curr Biol **15:** 1899–1911

Hudson A (1999) Axioms and axes in leaf formation? Curr Opin Plant Biol **2:** 56–60

Ilegems M, Douet V, Meylan-Bettex M, Uyttewaal M, Brand L, Bowman

JL, Stieger PA (2010) Interplay of auxin, KANADI and class III HD-ZIP transcription factors in vascular tissue formation. Development **137:** 975–984

Izhaki A, Bowman JL (2007) KANADI and class III HD-Zip gene families regulate embryo patterning and modulate auxin flow during embryogenesis in *Arabidopsis*. Plant Cell **19:** 495–508

Kidner CA, Timmermans MC (2007) Mixing and matching pathways in leaf polarity. Curr Opin Plant Biol **10:** 13–20

Lee BH, Ko JH, Lee S, Lee Y, Pak JH, Kim JH (2009) The Arabidopsis *GRF-INTERACTING FACTOR* gene family performs an overlapping function in determining organ size as well as multiple developmental properties. Plant Physiol **151:** 655–668

Li H, Xu L, Wang H, Yuan Z, Cao X, Yang Z, Zhang D, Xu Y, Huang H (2005) The putative RNA-dependent RNA polymerase *RDR6* acts synergistically with *ASYMMETRIC LEAVES1* and *2* to repress *BREVIPEDICELLUS* and MicroRNA165/166 in *Arabidopsis* leaf development. Plant Cell **17:** 2157–2171

Mattsson J, Sung ZR, Berleth T (1999) Responses of plant vascular systems to auxin transport inhibition. Development **126:** 2979–2991

McConnell JR, Barton MK (1998) Leaf polarity and meristem formation in *Arabidopsis*. Development **125:** 2935–2942

Pekker I, Alvarez JP, Eshed Y (2005) Auxin response factors mediate *Arabidopsis* organ asymmetry via modulation of KANADI activity. Plant Cell **17:** 2899–2910

Petrásek J, Mravec J, Bouchard R, Blakeslee JJ, Abas M, Seifertová D, Wisniewska J, Tadele Z, Kubes M, Covanová M, et al (2006) PIN proteins perform a rate-limiting function in cellular auxin efflux. Science **312:** 914–918

Poethig RS, Sussex IM (1985) The developmental morphology and growth dynamics of the tobacco leaf. Planta **165:** 170–184

Qi Y, Sun Y, Xu L, Xu Y, Huang H (2004) *ERECTA* is required for protection against heat-stress in the *AS1/AS2* pathway to regulate adaxial-abaxial leaf polarity in *Arabidopsis*. Planta **219:** 270–276

Reinhardt D, Frenz M, Mandel T, Kuhlemeier C (2005) Microsurgical and laser ablation analysis of leaf positioning and dorsoventral patterning in tomato. Development **132:** 15–26

Reinhardt D, Mandel T, Kuhlemeier C (2000) Auxin regulates the initiation and radial position of plant lateral organs. Plant Cell **12:** 507–518

Sarojam R, Sappl PG, Goldshmidt A, Efroni I, Floyd SK, Eshed Y, Bowman JL (2010) Differentiating *Arabidopsis* shoots from leaves by combined YABBY activities. Plant Cell **22:** 2113–2130

Scanlon MJ (2003) The polar auxin transport inhibitor *N*-1-naphthylphthalamic acid disrupts leaf initiation, KNOX protein regulation, and formation of leaf margins in maize. Plant Physiol **133:** 597–605

Scarpella E, Marcos D, Friml J, Berleth T (2006) Control of leaf vascular patterning by polar auxin transport. Genes Dev **20:** 1015–1027

Sussex IM (1954) Experiments on the cause of dorsaiventrality in leaves. Nature **174:** 351–352

Sussex IM (1955) Morphogenesis in *Solanum tuberosum* L: experiment investigation of leaf dorsoventrality and orientation in the juvenile shoot. Phytomorphology **5:** 286–300

Szakonyi D, Moschopoulos A, Byrne ME (2010) Perspectives on leaf dorsoventral polarity. J Plant Res **123:** 281–290

Ulmasov T, Murfett J, Hagen G, Guilfoyle TJ (1997) Aux/IAA proteins repress expression of reporter genes containing natural and highly active synthetic auxin response elements. Plant Cell **9:** 1963–1971

Vanneste S, Friml J (2009) Auxin: a trigger for change in plant development. Cell **136:** 1005–1016

Waites R, Hudson A (1995) *phantastica*: a gene required for dorsoventrality of leaves in *Antirrhinum majus*. Development **121:** 2143–2154

Woodward AW, Bartel B (2005) Auxin: regulation, action, and interaction. Ann Bot (Lond) **95:** 707–735

Wu G, Lin WC, Huang T, Poethig RS, Springer PS, Kerstetter RA (2008) KANADI1 regulates adaxial-abaxial polarity in *Arabidopsis* by directly repressing the transcription of *ASYMMETRIC LEAVES2*. Proc Natl Acad Sci USA **105:** 16392–16397

Xu L, Shen WH (2008) Polycomb silencing of *KNOX* genes confines shoot stem cell niches in *Arabidopsis*. Curr Biol **18:** 1966–1971

Xu L, Xu Y, Dong A, Sun Y, Pi L, Xu Y, Huang H (2003) Novel *as1* and *as2* defects in leaf adaxial-abaxial polarity reveal the requirement for *ASYMMETRIC LEAVES1* and *2* and *ERECTA* functions in specifying leaf adaxial identity. Development **130:** 4097–4107

Xu L, Yang L, Huang H (2007) Transcriptional, post-transcriptional and post-translational regulations of gene expression during leaf polarity formation. Cell Res **17:** 512–519

Zgurski JM, Sharma R, Bolokoski DA, Schultz EA (2005) Asymmetric auxin response precedes asymmetric growth and differentiation of *asymmetric leaf1* and *asymmetric leaf2 Arabidopsis* leaves. Plant Cell **17:** 77–91

Zhao Y, Christensen SK, Fankhauser C, Cashman JR, Cohen JD, Weigel D, Chory J (2001) A role for flavin monooxygenase-like enzymes in auxin biosynthesis. Science **291:** 306–309